

1 **Title**

2 The Boundary-Expressed *EPIDERMAL PATTERNING FACTOR-LIKE2* Gene
3 Encoding a Signaling Peptide Promotes Cotyledon Growth during *Arabidopsis thaliana*
4 Embryogenesis

5

6 **Authors**

7 Rina Fujihara¹, Naoyuki Uchida^{2,3}, Toshiaki Tameshige^{4,5}, Nozomi Kawamoto^{6,†}, Yugo
8 Hotokezaka⁷, Takumi Higaki⁸, Rüdiger Simon⁶, Keiko U Torii^{3,9}, Masao Tasaka¹, and
9 Mitsuhiro Aida^{8,*}

10

11 **Affiliations**

12 ¹Graduate School of Biological Sciences, Nara Institute of Science and Technology,
13 8916-5 Takayama, Ikoma 630-0192, Japan

14 ²Center for Gene Research, Nagoya University, Furo-cho, Chikusa-ku, Nagoya, Aichi
15 464-8602, Japan

16 ³Institute of Transformative Bio-Molecules (ITbM), Nagoya University, Furo-cho,
17 Chikusa-ku, Nagoya, Aichi 464-8601, Japan

18 ⁴Kihara Institute for Biological Research, Yokohama City University, 641-12 Maioka,
19 Totsuka-ku, Yokohama, Kanagawa 244-0813, Japan

20 ⁵Department of Biology, Faculty of Science, Niigata University, 8050 Ikarashi 2-no-cho,
21 Nishi-ku, Niigata, Niigata 950-2181, Japan

22 ⁶Institute for Developmental Genetics, Heinrich-Heine University, University Street 1,
23 D-40225 Düsseldorf, Germany; Cluster of Excellence on Plant Sciences (CEPLAS),
24 University Street 1, D-40225 Düsseldorf, Germany

25 ⁷Faculty of Science, Kumamoto University, 2-39-1 Kurokami, Chuo-ku, Kumamoto
26 860-8555, Japan

27 ⁸International Research Organization for Advanced Science and Technology (IROAST),
28 Kumamoto University, 2-39-1 Kurokami, Chuo-ku, Kumamoto 860-8555, Japan

29 ⁹Howard Hughes Medical Institute and Department of Molecular Biosciences,
30 University of Texas at Austin, Austin, TX 78712, USA

31

32 ***Corresponding Author**

33 Mitsuhiro Aida

34 Address: International Research Organization for Advanced Science and Technology
35 (IROAST), Kumamoto University, 2-39-1 Kurokami, Chuo-ku, Kumamoto 860-8555,

36 Japan

37 Phone/FAX: +81-96-342-3402

38 E-mail address: m-aida@kumamoto-u.ac.jp

39

40 **Running Title**

41 The Boundary Gene *EPFL2* in Cotyledon Development

42

43 **Abbreviations**

44 *EPIDERMAL PATTERNING FACTOR-LIKE: EPFL*

45 *Arabidopsis thaliana: A. thaliana*

46 Landsberg *erecta: Ler*

47 Columbia: Col

48 β -glucuronidase: *GUS*

49 clustered regularly interspaced short palindromic repeat: CRISPR

50 CRISPR associated protein 9: Cas9

51 Green Fluorescent Protein: GFP

52 ERECTA: ER

53 ERECTA-LIKE: ERL

54 a. u.: arbitrary unit

55

56 **Footnotes**

57 †Present Address: Division of Plant Environmental Responses, National Institute for
58 Basic Biology, Nishigonaka 38, Myodaiji, Okazaki, 444-8585, Aichi, Japan

59

60 **Abstract**

61 The shoot organ boundaries have important roles in plant growth and morphogenesis. It
62 has been reported that a gene encoding a cysteine-rich secreted peptide of the
63 EPIDERMAL PATTERNING FACTOR-LIKE (EPFL) family, *EPFL2*, is expressed in
64 the boundary domain between the two cotyledon primordia of *Arabidopsis thaliana*
65 embryo. However, its developmental functions remain unknown. This study aimed to
66 analyze the role of *EPFL2* during embryogenesis. We found that cotyledon growth was
67 reduced in its loss-of-function mutants, and this phenotype was associated with the
68 reduction of auxin response peaks at the tips of the primordia. The reduced cotyledon
69 size of the mutant embryo recovered in germinating seedlings, indicating the presence
70 of a factor that acted redundantly with *EPFL2* to promote cotyledon growth in late
71 embryogenesis. Our analysis indicates that the boundary domain between the cotyledon
72 primordia acts as a signaling center that organizes auxin response peaks and promotes
73 cotyledon growth.

74

75 **Keywords**

76 auxin, boundary, cotyledon development, embryogenesis, signaling peptide

77

78 **Introduction**

79 The growth and morphogenesis of plant organs are manifested by the interactions
80 between each organ and surrounding regions. An important class of developmental
81 domains that affects the shoot organ development is the boundary domain, which is
82 generated between the adjacent shoot organ primordia or between the shoot meristem
83 and organ primordium (Aida and Tasaka 2006). The boundary domain is characterized
84 by the expression of specific regulatory genes and differential activities of plant
85 hormones. It also plays pivotal roles in shoot meristem activity regulation, adjacent
86 shoot organ separation, and new shoot meristem formation (Hepworth and Pautot 2015;
87 Žádníková and Simon 2014).

88 The interactions between the different developmental domains are partly mediated by
89 signaling molecules, such as hormones and small peptides. Among these molecules, the
90 EPIDERMAL PATTERNING FACTOR-LIKE (EPFL) family of secreted cysteine-rich
91 proteins is involved in various developmental pathways, including epidermal cell
92 patterning, inflorescence architecture, and lateral shoot organ patterning (Tameshige et
93 al. 2017; Torii 2012). Several studies have shown that one of the genes encoding an
94 EPFL family member, *EPFL2*, is specifically expressed in the boundary domains of
95 various shoot organs and regulates shoot meristem size, leaf and ovule positioning, and
96 leaf margin morphogenesis (Kawamoto et al. 2020; Kosentka et al. 2019; Tameshige et
97 al. 2016). The boundary-specific expression of this gene has also been reported during
98 embryogenesis (Kosentka et al. 2019), in which a series of patterning and growth events
99 occur to establish the basic body plan (Palovaara et al. 2016).

100 Although the functions of *EPFL2* in the boundary domain have been investigated in
101 various developmental contexts, the role of this gene in embryogenesis is unknown.
102 This study aimed to investigate the function of *EPFL2* during embryogenesis. The
103 expression analysis was extended to earlier embryonic stages relative to the previous
104 report by Kosentka et al. (2019), and we found that this gene was expressed in the

105 embryo apex before the initiation of cotyledon primordia. The analysis of loss-of-
106 function mutants of *EPFL2* showed that the size of the cotyledon primordia was
107 significantly reduced, and the activity of an auxin response marker, *DR5*, was also
108 significantly decreased. The results suggest that the boundary domain in the embryo
109 apex plays an important role in promoting the growth of adjacent cotyledons.

110

111 **Materials and Methods**

112 **Plant materials and growth conditions**

113 The *A. thaliana* accessions *Ler* and *Col* were used as the wild-type strains. The
114 *EPFL2pro::GUS* reporter (*Col* background), transposon insertion allele *epfl2-1* (*Ler*
115 background), and CIRSPR/Cas9-induced alleles *epfl2-2* and *epfl2-3* (*Col* background)
116 were described previously (Kawamoto et al. 2020; Tameshige et al. 2016). For the
117 analysis of *DR5rev::GFP* (Friml et al. 2003), the *epfl2-1* allele was backcrossed to *Col*
118 seven times and then crossed with the reporter line of the *Col* background (Tameshige
119 et al. 2016). The plants were grown as described previously (Takeda et al. 2011).

120 **Microscopy**

121 GUS staining was done as previously described (Aida et al. 2020). For the visualization
122 of the embryo morphology, the ovules were cleared as described previously (Aida et al.
123 1999), and their stages were determined according to Jürgens and Mayer (1994). To
124 measure the length and cell number of the cotyledons in germinating seedlings, the
125 seeds were first imbibed on wet filter paper for three days at 4 °C in the dark; then, they
126 were incubated in a growth chamber at 23 °C under constant white light for 24 h. After
127 removing the seed coat, the cotyledons were excised and directly mounted in a clearing
128 solution (8 g of chloral hydrate, 1 ml of glycerol, and 2 ml of water). The measurements
129 were carried out in the palisade layer. For the analysis of *DR5rev::GFP*, the embryos
130 were cleared as described previously (Imoto et al. 2021), and the confocal images were
131 taken using LSM 5 Live (Zeiss [Oberkochen, Germany]). Because the signal intensities
132 were generally much higher in the root than in the cotyledons (~5.7 fold), a pair of
133 images with different fixed values of Main Gain parameter (50 and 25 for cotyledons
134 and root, respectively) was independently collected for each embryo to avoid the
135 saturation of the signals of interest. To quantify the GFP signals, the average
136 background value in a small area within the embryo was subtracted from the maximum
137 signal value in the protoderm of the cotyledon tips or that in the outermost columella
138 root cap cells. The image and statistical analyses were performed using Fiji (Schindelin
139 et al. 2012) and R (version 3.6.1; The R Foundation for Statistical Computing Platform),
140 respectively.

141

142 **Results**

143 **Expression of *EPFL2* during embryogenesis**

144 We first examined the expression patterns of the *EPFL2* gene in the embryo using a
145 GUS reporter. The GUS activity was first detected in a small area of the apical region at
146 the mid-globular stage (Figure 1A). The embryos with an oblique view indicate that the
147 expression was initiated as a pair of asymmetric spots (Figure 1A, inset). At the heart
148 stage, the expression was detected in the boundary domain between the two cotyledon

149 primordia (Figure 1B, C), and this expression pattern continued in the later stages
150 (Figure 1D). Within the boundary domain, the GUS activity was much stronger in the
151 periphery than in the center (Figure 1C). These results indicate that the expression of
152 *EPFL2* starts before the cotyledon initiation and continues in the boundary domain in
153 the later stages of embryogenesis.

154 ***EPFL2* is required for cotyledon growth during embryogenesis**

155 To investigate the function of *EPFL2*, we examined the effect of its loss-of-function
156 mutations on embryo development. The null allele *epfl2-1* (Tameshige et al. 2016),
157 which was generated in the *Ler* background, did not display obvious morphological
158 defects up to the globular stage (Figure 2A, B). However, after the heart stage, the
159 cotyledon primordia were shorter compared to those of the wild-type *Ler* (Figure 2C,
160 D). We quantified this phenotype and found that the height of the cotyledon primordia
161 relative to that of the rest of the embryo (referred to as cotyledon height and axis height,
162 respectively; Figure 2E) was smaller in *epfl2-1* than in *Ler* (Figure 2F). The reduction
163 of the cotyledon height was the most prominent when the axis height was 51–100 μm
164 (47.7 % reduction; Figure 2G), and it became less as the axis height increased (33.7 %
165 in 101–150 μm and 32.2 % in 151–200 μm ; Figure 2G).

166 We also analyzed *epfl2-2* and *epfl2-3*, which are CRIPR/Cas9-induced alleles in the
167 *Col* background, and they both showed similar reduction in cotyledon height (Figure 2H,
168 I), although their phenotypes were milder compared to that of the *Ler* allele *epfl2-1* (e.g.,
169 33.9 % and 23.0 % reduction in *epfl2-2* and *epfl2-3*, respectively, for embryos with 51–
170 100 μm axis height range). The deduced amino acid sequence produced from *epfl2-2*
171 completely lacks a mature peptide (Kawamoto et al. 2020), indicating that this allele is
172 null, similar to *epfl2-1*. Therefore, the observed difference in the phenotypic severity of
173 *epfl2-1* and *epfl2-2* is likely due to their difference in genetic background rather than
174 that in allele strength. Besides the size reduction in cotyledon primordia, no obvious
175 abnormality was found in any of the *epfl2* mutant alleles. Our analysis shows that
176 *EPFL2* is required to promote cotyledon growth during embryogenesis.

177 **The reduction in cotyledon size of *epfl2* mutants was rescued in germinating** 178 **seedlings**

179 We also examined the early seedling phenotypes of *epfl2* mutants. The shape and size of
180 the cotyledons in *epfl2* mutants were indistinguishable from those of the wild type
181 (Figure 3A, B). The formation of leaves also occurred normally, except that the leaf
182 margins lacked serrations, as reported previously (Tameshige et al. 2016). The
183 quantification of the length and cell number along the proximo-distal and lateral axes of
184 the cotyledons showed no significant reduction in these values in germinating, one-day-
185 old seedlings of the two *Col* alleles (Figure 2C, D). In *epfl2-3*, the size and cell number
186 along the proximo-distal axis were significantly greater than those of *Col*. Although the
187 reason for this allele-specific effect is unclear, our results show that neither of the *epfl2*
188 mutations caused the reduction in cotyledon size or cell number, indicating that the
189 reduced cotyledon growth in mutants during embryogenesis was rescued in germinating
190 seedlings.

191 ***EPFL2* is required to establish auxin response peaks at the cotyledon tips**
192 It has been established that the formation of auxin response peaks (also called auxin
193 maxima) is essential for proper cotyledon development (Benková et al. 2003). Therefore,
194 we analyzed the patterns of the auxin response reporter, *DR5rev::GFP*, in *epfl2*
195 embryos (see Materials and Methods). In the wild type, the GFP signals were detected
196 as a pair of apical spots and single basal spot, each of which corresponds to the *DR5*
197 activity at the two cotyledon tips and root tip, respectively (Figure 4A). In the wild type,
198 most embryos possessed two recognizable apical signals at the heart stage. However,
199 within a single embryo, the signal intensity was often different in each of the cotyledon
200 tips (arrowheads in Figure 4A). In contrast, the *epfl2* mutant embryos often lack
201 recognizable apical signals in one or both of the cotyledon tips (Figure 4B, C). The
202 intensity of the apical signals was significantly lower in *epfl2* than in the wild type
203 (60.9 % reduction; Figure 4D). In contrast to the reduction of the apical signals, the
204 *epfl2* mutant embryos did not show significant changes in the pattern or intensity of the
205 GFP signals in the root pole (Figure 4A, B, E). These results demonstrate that *EPFL2* is
206 required to establish auxin response peaks in the apical embryo, and are consistent with
207 the specific role for this gene in cotyledon development during embryogenesis.

208

209 Discussion

210 Our analysis demonstrates that *EPFL2* is required to promote cotyledon growth during
211 embryogenesis. The phenotype of the mutant can be clearly observed from the heart
212 stage, an early stage in cotyledon formation. This result is consistent with the early
213 onset of *EPFL2* expression at the globular stage, indicating that the gene is required for
214 cotyledon growth from its initiation. Our results are also consistent with the non-cell
215 autonomous action of the *EPFL2* gene in cotyledon development, indicating that the
216 cotyledon boundary domain provides a growth-promoting signal by producing the
217 secreted peptide.

218 The best candidate receptors for *EPFL2* are the *ERECTA* family proteins *ER*, *ERL1*,
219 and *ERL2*, which constitute a subgroup of leucine-rich repeat receptor-like kinases
220 (*LRR-RLKs*; reviewed by Shpak [2013]). All these proteins have been shown to bind to
221 *EPFL2* both *in vivo* and *in vitro*, and genetic studies support that *EPFL2* is a ligand for
222 the *ER* family proteins in leaf tooth growth and ovule patterning (Kawamoto et al. 2020;
223 Tameshige et al. 2016). In addition, the genes for these receptors are all expressed in a
224 broad region that includes the cotyledon primordia in the embryo and are redundantly
225 required for cotyledon growth (Chen and Shpak 2014). To demonstrate that *EPFL2* is a
226 ligand for the *ER* family proteins in cotyledon development, it would be important to
227 test whether the growth-promoting activity of the receptors requires the binding of the
228 secreted peptide. In this regard, it would be also important to test whether the observed
229 difference in the severity of the phenotype between the *Ler* and *Col* alleles of *epfl2*
230 involves the lack of a fully functional *ER* allele in the *Ler* background (Torii et al. 1996).

231 An interesting property of *epfl2* mutants is that the reduction in cotyledon size is only
232 apparent in the embryo, and their phenotype recovers by early seedling stage. These
233 results indicate that the *EPFL2*-dependent growth signal is only essential in the early
234 stages of cotyledon development, and the loss of its activity is compensated by other
235 redundant factors. A candidate for such factor is *EPFL1*, an *EPFL* family member that

236 is also expressed in the boundary domain of the cotyledon primordia (Kosentka et al.
237 2019). In postembryonic development, *EPFL1* is expressed along the boundary between
238 the shoot meristem and leaf primordia and acts redundantly with *EPFL2* and other
239 *EPFL* family members to regulate the shoot meristem size and leaf initiation (Kosentka
240 et al. 2019). Thus, it is likely that the boundary-dependent growth promotion of the
241 cotyledons is supported by multiple redundant factors.

242 The formation of auxin response peaks is known to be a common key factor in
243 promoting the growth of various organs and tissues (Benková et al. 2003; Bilborough
244 et al. 2011; Galbiati et al. 2013; Heisler et al. 2005), and the observed reduction in the
245 *DR5* activity at the cotyledon tips of *epfl2* mutants is consistent with this view. However,
246 whether *EPFL2*-dependent signals directly activate the auxin response is still unclear
247 and requires further investigation. It is also important to note that the effect of *EPFL2*
248 on auxin response peaks in the cotyledon tips is significantly different from other
249 developmental contexts. In leaf margin morphogenesis, for example, *EPFL2* rather
250 affects the auxin response negatively and restricts the domain of *DR5* expression to the
251 narrow region within the leaf tooth. In turn, the auxin peak in the tooth represses the
252 *EPFL2* expression, and this mutual repression ensures the spatially complementary
253 patterns of the two factors (Tameshige et al. 2016). A similar negative effect of *EPFL2*
254 on auxin response has also been reported for the vegetative shoot apex (Kosentka et al.
255 2019). The opposite effects of *EPFL2* on auxin response (positive effect in cotyledons
256 vs negative effect in leaf margins and shoot apices) but the same developmental output
257 (primordium growth promotion) is seemingly paradoxical. However, this can be
258 explained by assuming that the primordium growth is driven by the differential
259 distribution of auxin response rather than its absolute strength—a view that has been
260 shown in leaf margin development (Bilborough et al. 2011). A comparative analysis of
261 how *EPFL2*-dependent signal regulates the *DR5* expression in different developmental
262 contexts described above will shed light on the variations in the mechanism to establish
263 auxin response peaks by the same signaling peptide.

264

265 **Acknowledgements**

266 We thank Maki Niidome, Mie Matsubara, Shoko Nagame, and Kazuko Onga for
267 technical assistance. This work was supported by MEXT KAKENHI (Grant No.
268 17H06476 to KUT, 24114009, 18H04842, 20H04889 to MA); JSPS KAKENHI (Grant
269 No. JP21H02503 to NU, 16K07401 to MA); WPI-ITbM operational funds to NU and
270 KUT; IROAST operational funds to TH and MA; Takeda Science Foundation to MA.

271

272 **References**

- 273 Aida M, Ishida T and Tasaka M (1999) Shoot apical meristem and cotyledon formation
274 during *Arabidopsis* embryogenesis: interaction among the *CUP-SHAPED*
275 *COTYLEDON* and *SHOOT MERISTEMLESS* genes. *Development* 126: 1563-
276 1570
- 277 Aida M and Tasaka M (2006) Genetic control of shoot organ boundaries. *Curr Opin*
278 *Plant Biol* 9: 72-77
- 279 Aida M, Tsubakimoto Y, Shimizu S, Ogisu H, Kamiya M, Iwamoto R, Takeda S, Karim
280 MR, Mizutani M, Lenhard M et al. (2020) Establishment of the embryonic shoot

- 281 meristem involves activation of two classes of genes with opposing functions for
282 meristem activities. *Int J Mol Sci* 21: 5864
- 283 Benková E, Michniewicz M, Sauer M, Teichmann T, Seifertova D, Jürgens G and Friml
284 J (2003) Local, efflux-dependent auxin gradients as a common module for plant
285 organ formation. *Cell* 115: 591-602
- 286 Biltsborough GD, Runions A, Barkoulas M, Jenkins HW, Hasson A, Galinha C, Laufs P,
287 Hay A, Prusinkiewicz P and Tsiantis M (2011) Model for the regulation of
288 *Arabidopsis thaliana* leaf margin development. *Proc Natl Acad Sci U S A* 108:
289 3424-3429
- 290 Chen MK and Shpak ED (2014) *ERECTA* family genes regulate development of
291 cotyledons during embryogenesis. *FEBS Lett* 588: 3912-3917
- 292 Friml J, Vieten A, Sauer M, Weijers D, Schwarz H, Hamann T, Offringa R and Jürgens
293 G (2003) Efflux-dependent auxin gradients establish the apical-basal axis of
294 *Arabidopsis*. *Nature* 426: 147-153
- 295 Galbiati F, Sinha Roy D, Simonini S, Cucinotta M, Ceccato L, Cuesta C, Simaskova M,
296 Benkova E, Kamiuchi Y, Aida M et al. (2013) An integrative model of the
297 control of ovule primordia formation. *Plant J* 76: 446-455
- 298 Heisler MG, Ohno C, Das P, Sieber P, Reddy GV, Long JA and Meyerowitz EM (2005)
299 Patterns of auxin transport and gene expression during primordium development
300 revealed by live imaging of the *Arabidopsis* inflorescence meristem. *Curr Biol*
301 15: 1899-1911
- 302 Hepworth SR and Pautot VA (2015) Beyond the divide: boundaries for patterning and
303 stem cell regulation in plants. *Front Plant Sci* 6: 1052
- 304 Imoto A, Yamada M, Sakamoto T, Okuyama A, Ishida T, Sawa S and Aida M (2021) A
305 ClearSee-based clearing protocol for 3D visualization of *Arabidopsis thaliana*
306 embryos. *Plants* 10: 190
- 307 Jürgens G and Mayer U (1994) *Arabidopsis*. In: (Bard, J. ed) *Embryos: Color Atlas of*
308 *Development* Wolfe, London pp. 7-21.
- 309 Kawamoto N, Del Carpio DP, Hofmann A, Mizuta Y, Kurihara D, Higashiyama T,
310 Uchida N, Torii KU, Colombo L, Groth G et al. (2020) A peptide pair
311 coordinates regular ovule initiation patterns with seed number and fruit size.
312 *Curr Biol* 30: 4352-4361.e4354
- 313 Kosentka PZ, Overholt A, Maradiaga R, Mitoubsi O and Shpak ED (2019) EPFL
314 signals in the boundary region of the SAM restrict its size and promote leaf
315 initiation. *Plant Physiol* 179: 265-279
- 316 Palovaara J, de Zeeuw T and Weijers D (2016) Tissue and organ initiation in the plant
317 embryo: a first time for everything. *Annu Rev Cell Dev Biol* 32: 47-75
- 318 Schindelin J, Arganda-Carreras I, Frise E, Kaynig V, Longair M, Pietzsch T, Preibisch
319 S, Rueden C, Saalfeld S, Schmid B et al. (2012) Fiji: an open-source platform
320 for biological-image analysis. *Nat Methods* 9: 676-682
- 321 Shpak ED (2013) Diverse roles of *ERECTA* family genes in plant development. *J Integr*
322 *Plant Biol* 55: 1238-1250
- 323 Takeda S, Hanano K, Kariya A, Shimizu S, Zhao L, Matsui M, Tasaka M and Aida M
324 (2011) CUP-SHAPED COTYLEDON1 transcription factor activates the
325 expression of *LSH4* and *LSH3*, two members of the ALOG gene family, in shoot

326 organ boundary cells. *Plant J* 66: 1066-1077
327 Tameshige T, Ikematsu S, Torii KU and Uchida N (2017) Stem development through
328 vascular tissues: EPFL-ERECTA family signaling that bounces in and out of
329 phloem. *J Exp Bot* 68: 45-53
330 Tameshige T, Okamoto S, Lee JS, Aida M, Tasaka M, Torii KU and Uchida N (2016) A
331 secreted peptide and its receptors shape the auxin response pattern and leaf
332 margin morphogenesis. *Curr Biol* 26: 2478-2485
333 Torii KU (2012) Mix-and-match: ligand-receptor pairs in stomatal development and
334 beyond. *Trends Plant Sci* 17: 711-719
335 Torii KU, Mitsukawa N, Oosumi T, Matsuura Y, Yokoyama R, Whittier RF and
336 Komeda Y (1996) The Arabidopsis *ERECTA* gene encodes a putative receptor
337 protein kinase with extracellular leucine-rich repeats. *Plant Cell* 8: 735-746
338 Žádníková P and Simon R (2014) How boundaries control plant development. *Curr*
339 *Opin Plant Biol* 17: 116-125
340

341 **Figure Legends**

342 **Figure 1.** Expression patterns of *EPFL2pro::GUS*. Wild-type embryos at the mid-
343 globular (A), mid-heart (B and C), and mid-torpedo (D) stages. Frontal (A, B, and D)
344 and top (C) views. The inset in (A) shows an embryo with two asymmetric spots of
345 GUS activity (arrowheads) on oblique view. The asterisks indicate the cotyledon
346 primordia. Scale bars = 50 μ m.

347 **Figure 2.** Embryonic phenotype of *epfl2* mutants. (A to D) Cleared embryos at the mid-
348 globular stage of wild-type *Ler* (A) and *epfl2-1* (B) and those at the late-heart stage
349 of *Ler* (C) and *epfl2-1* (D). (E) Quantification of the cotyledon size. The height of the
350 cotyledon (c) and axis (a) was measured. The axis refers to the region that spans the
351 shoot apex and the root tip. (F) Relationship between the axis and cotyledon height. The
352 open circles and black dots represent the individual embryos of *Ler* and *epfl2-1*,
353 respectively. (G) Cotyledon height of embryos with three classes of different axis height.
354 The open and closed bars represent *Ler* and *epfl2-1*, respectively. (H) Relationship
355 between the axis and cotyledon height of wild-type *Col* vs *epfl2-2* (left panel) and *Col*
356 vs *epfl2-3* (right panel). The open circles and black dots represent the individual
357 embryos of *Col* and mutants, respectively. Each mutant data set is compared to the same
358 data set of *Col*. (I) Cotyledon height of embryos with three classes of different axis
359 height. The open, closed, and gray bars represent *Col*, *epfl2-2*, and *epfl2-3*,
360 respectively. Scale bars = 20 μ m in A and B and 50 μ m in C and D. The three classes
361 with different axis height roughly correspond to heart (51–100 μ m), early-torpedo (101–
362 150 μ m), and mid-torpedo (151–200 μ m) stages according to Jürgens and Mayer (1994).
363 The error bars represent the standard deviation. The double asterisks indicate the
364 significant differences between each mutant and wild-type control ($p < 0.01$; Welch's t-
365 test for G and Dunnett's test for I). The sample sizes for each measurement are
366 described in Supplementary File 1.

367 **Figure 3.** Seedling phenotype of *epfl2* mutants. (A and B) Top views of seven-day-old
368 wild-type *Col* and *epfl2-2* mutant seedlings. (C) Length (left) and cell number (right) of

369 cotyledons along the proximo-distal axis in one-day-old wild-type Col and *epfl2* mutant
370 seedlings. (D) Length (left) and cell number (right) of cotyledons along the lateral axis
371 in one-day-old Col and *epfl2* mutants. The single and double asterisks indicate the
372 significant differences between each mutant and wild-type control ($p < 0.05$ and $p <$
373 0.01 , respectively; Dunnett's test for C and D). Scale bars = 1 mm. The sample sizes for
374 each measurement are described in Supplementary File 1.

375 **Figure 4.** Expression of *DR5rev::GFP*. (A and B) Patterns of *DR5rev::GFP* in the wild
376 type (A) and *epfl2* (B) backgrounds. The whole views of embryos are shown in the
377 middle panels with cell wall staining (magenta) and GFP signals (cyan), with top and
378 bottom panels showing color-coded signal intensities of GFP at the cotyledon (top) and
379 root (bottom) tips of the same embryos. The arrowheads indicate the recognizable GFP
380 signals at the cotyledon tip. (C) Distribution of embryos with different numbers of
381 recognizable apical GFP signals. The open and closed circles represent the individual
382 embryos of wild type and *epfl2*, respectively. (D and E) GFP signal intensity of each
383 genotype in the cotyledon (D) and root (E) tips. The double asterisks indicate the
384 significant differences between the mutant and Col ($p < 0.01$, Brunner–Munzel test for
385 C and Welch's t-test for D and E). Scale bars = 50 μm . The sample sizes for each
386 measurement are described in Supplementary File 1.

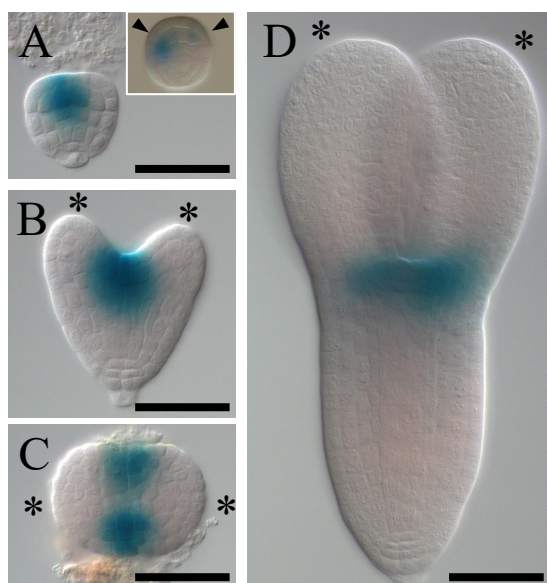


Figure 1

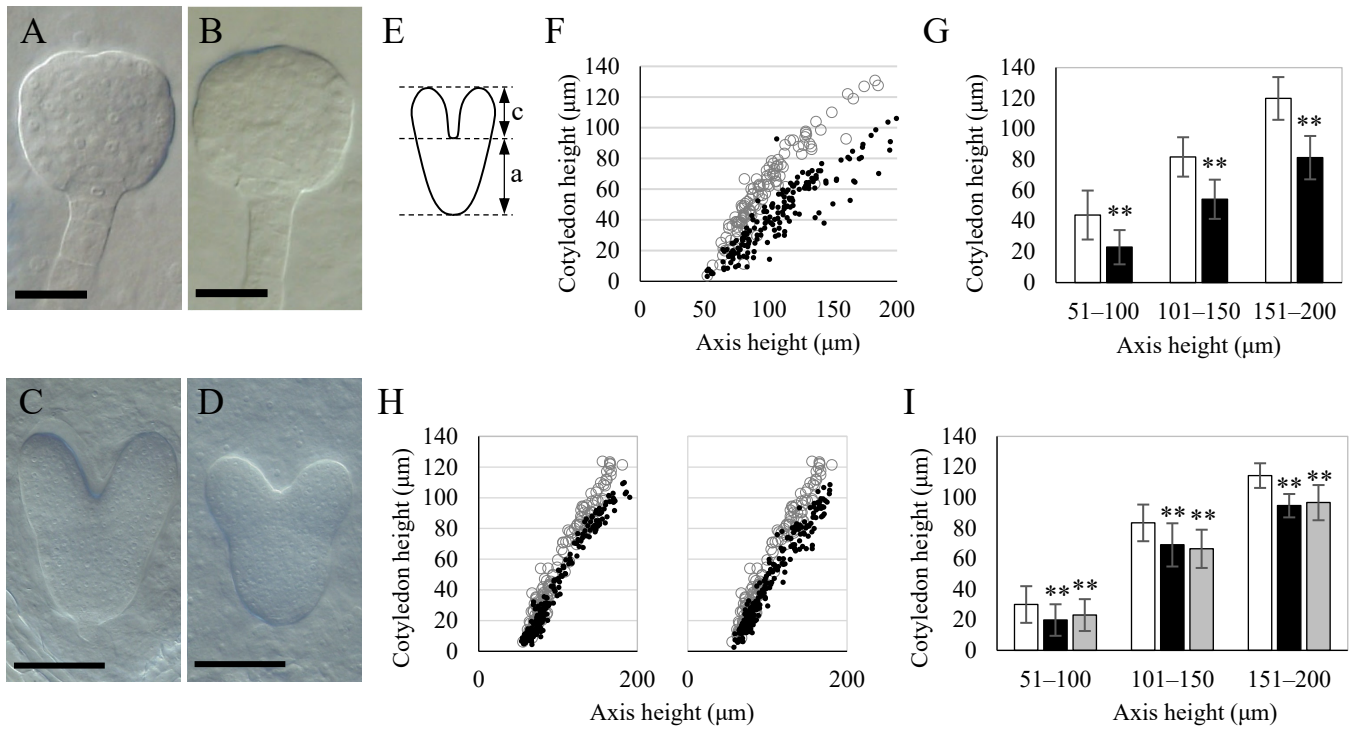


Figure 2

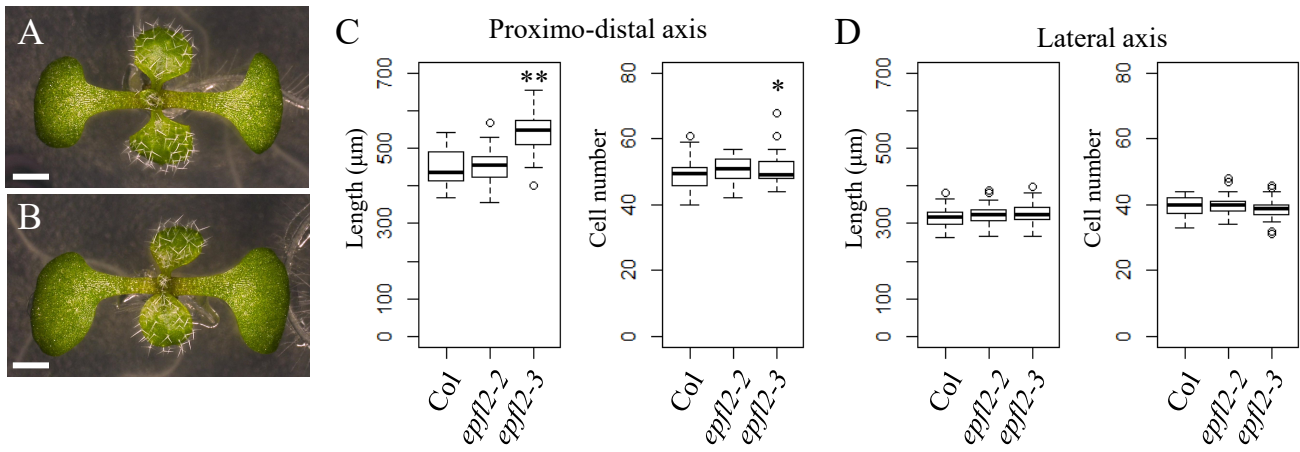


Figure 3

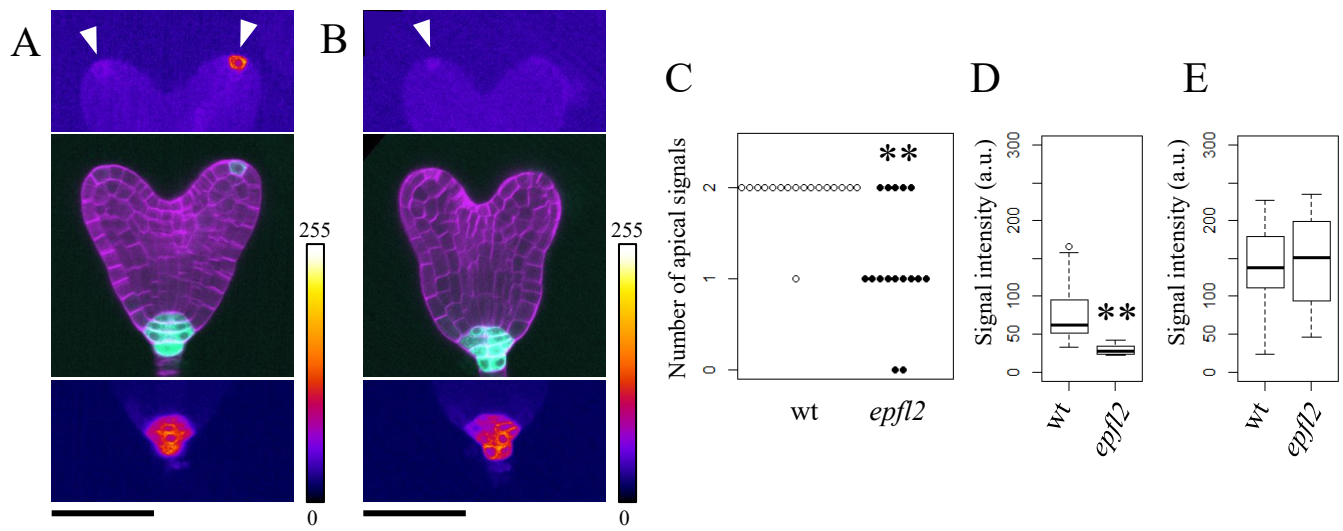


Figure 4